Evolution of multicellularity coincided with increased diversification of cyanobacteria and the Great Oxidation Event

Bettina E. Schirrmeister[a,1,2], Jurriaan M. de Vos[b], Alexandre Antonelli[c], and Homayoun C. Bagheri[a]

[a]Institute of Evolutionary Biology and Environmental Studies, University of Zurich, CH-8057 Zurich, Switzerland; [b]Institute of Systematic Botany, University of Zurich, CH-8008 Zurich, Switzerland; and [c]Gothenburg Botanical Garden and Department of Biological and Environmental Sciences, University of Gothenburg, SE 405 30 Gothenburg, Sweden

Edited by Stjepko Golubic, Boston University, Boston, MA, and accepted by the Editorial Board December 13, 2012 (received for review June 15, 2012)

Cyanobacteria are among the most diverse prokaryotic phyla, with morphotypes ranging from unicellular to multicellular filamentous forms, including those able to terminally (i.e., irreversibly) differentiate in form and function. It has been suggested that cyanobacteria raised oxygen levels in the atmosphere around 2.45–2.32 billion y ago during the Great Oxidation Event (GOE), hence dramatically changing life on the planet. However, little is known about the temporal evolution of cyanobacterial lineages, and possible interplay between the origin of multicellularity, diversification of cyanobacteria, and the rise of atmospheric oxygen. We estimated divergence times of extant cyanobacterial lineages under Bayesian relaxed clocks for a dataset of 16S rRNA sequences representing the entire known diversity of this phylum. We tested whether the evolution of multicellularity overlaps with the GOE, and whether multicellularity is associated with significant shifts in diversification rates in cyanobacteria. Our results indicate an origin of cyanobacteria before the rise of atmospheric oxygen. The evolution of multicellular forms coincides with the onset of the GOE and an increase in diversification rates. These results suggest that multicellularity could have played a key role in triggering cyanobacterial evolution around the GOE.

early life | major transitions | prokaryotic phylogenetics | molecular clock

Cyanobacteria are one of the morphologically most diverse groups of prokaryotic organisms. Growth forms range from uni- to multicellular, and can include levels of reversible or terminal (i.e., irreversible) cell differentiation. These diverse growth strategies have enabled cyanobacteria to inhabit almost every terrestrial and aquatic habitat on Earth. Cyanobacteria have traditionally been classified into five subsections according to their morphology (1, 2), where subsections I and II refer to unicellular species and subsections III–V describe multicellular species. Species belonging to subsections IV and V are able to produce terminally differentiated cells. Despite the usefulness of these subsections, molecular evidence shows that morphological and genetic diversity do not always coincide. Molecular phylogenies indicate that probably none of the five subsections is monophyletic (3, 4), and several transitions between uni- and multicellularity have taken place (5). According to the fossil record, various distinct morphotypes attributed to cyanobacteria were already present over 2 billion y ago (Bya) (6, 7). The phylum is thought to have existed as early as 2.45–2.32 Bya, based on the assumption that cyanobacteria were responsible for the accumulation of atmospheric oxygen levels, referred to as the Great Oxidation Event (GOE) (8–12). Despite the generally accepted time-frame for the rise of cyanobacteria, surprisingly little is known about when morphological innovations, such as multicellularity, first appeared. It is also unclear what influence, if any, these innovations may have had on the diversification of the phylum. The assumed link between the rise of atmospheric oxygen and cyanobacteria is also poorly understood: did the GOE closely follow the first appearance of cyanobacteria, or did it take place considerably later, in possible association with morphological innovations of the phylum?

There have been previous attempts to estimate the origin of cyanobacteria and their morphotypes (13–16). However, it is likely that a biased taxonomic choice, especially missing early branches of the cyanobacterial phylogeny, may have led to incomplete conclusions (17, 18). Phylogenetic evidence indicates that multicellularity evolved very early in the history of cyanobacteria, challenging the view that multicellularity is a derived condition in the phylum (5). Nonetheless, important questions remain: (*i*) When did cyanobacteria and their major clades evolve? (*ii*) When did multicellularity first appear? (*iii*) How are these transitions associated with the GOE around 2.45–2.32 Bya?

The far-reaching impact of the GOE cannot be emphasized enough: it changed Earth's history by enabling the evolution of aerobic life. Unlike other eubacterial phyla, cyanobacteria exhibit a well-studied fossil record (6, 7, 19, 20). However, fossil data are often limited and present only minimum age estimates of clades. Therefore, a combination of fossil data with molecular phylogenetic methods has been advocated (21–23). The use of carefully selected calibration priors for molecular-dating analyses can provide new insights into the temporal evolution of cyanobacteria and the early history of life. Presently, available genome data for cyanobacteria are biased toward unicellular taxa and do not sufficiently represent the known diversity of this phylum. Therefore, we reconstructed phylogenetic trees on the basis of 16S rRNA sequences, which have been carefully sampled based on phylogenetic disparity as described previously (5). We further estimated divergence times of cyanobacteria, and addressed different interpretations of the fossil record as calibration priors. We then evaluated whether the GOE coincided with the development of major cyanobacterial morphotypes present today. Finally, we tested for shifts in diversification rates, incorporating information on 281 species and 4,194 strains. Our results support theories of an early cyanobacterial origin toward the end of the Archean Eon, before 2.5 Bya. Evolution of multicellularity coincided with the onset of the GOE, and corresponded to a marked increase of diversification in cyanobacteria.

Author contributions: B.E.S., J.M.d.V., A.A., and H.C.B. designed research; B.E.S. and J.M.d.V. analyzed data; and B.E.S., J.M.d.V., A.A., and H.C.B. wrote the paper.

The authors declare no conflict of interest.

This article is a PNAS Direct Submission. S.G. is a guest editor invited by the Editorial Board.

Freely available online through the PNAS open access option.

Data deposition: The sequences reported in this paper have been deposited in the GenBank database (accession no. JX069960).

[1]Present address: School of Earth Sciences, University of Bristol, Bristol BS8 1RJ, United Kingdom.

[2]To whom correspondence should be addressed. E-mail: bettina.schirrmeister@bristol.ac.uk.

This article contains supporting information online at www.pnas.org/lookup/suppl/doi:10.1073/pnas.1209927110/-/DCSupplemental.

Results

Phylogenetic Analyses. To infer the early evolution of cyanobacteria, we reconstructed Bayesian phylogenetic trees using 16S rRNA sequence data. A phylogenomic approach would give misleading results, because available cyanobacterial genome sequences, to date, are heavily biased toward unicellular species. Moreover, the few multicellular species that have been fully sequenced are phylogenetically closely related, and a comparison of these species is unlikely to provide any information on the ancient origin of multicellularity in cyanobacteria (17). In a previous study (5), a phylogenetic tree of 1,220 cyanobacterial sequences was reconstructed from which a subset of taxa was sampled that represents the surveyed diversity of this phylum. Here we used this subset plus one strain (G40) that represents a potentially unique distinct species isolated by our group. Our unconstrained phylogenetic results (Fig. S1) agree with previous findings (3, 5, 15, 24, 25), which reject monophyly of several morphological groups previously described (1, 2). Furthermore, *Gloeobacter violaceus* is resolved as the sister group of all other cyanobacteria. Three major groups can be distinguished (clades E1, E2, and group AC) (Fig. 1, and Figs. S1 and S2), together representing the majority of cyanobacterial taxa living today. All groups have been defined previously (5), with clades E1 and E2 (subclades of E) including species of all morphological subsections. Species belonging to morphological subsections IV and V occur solely in E1. The group AC contains unicellular marine pico-phytoplankton (subsection I) as well as some undifferentiated multicellular species (subsection III).

Divergence Time Estimation. Divergence times along the cyanobacterial phylogeny were estimated under Bayesian relaxed molecular clocks using two different models of uncorrelated rate evolution (26). A lognormal distribution of rates has been shown to outperform a model with exponential rate distribution (26). Therefore, our first model assumed rates were lognormally distributed (uncorrelated lognormal, UCLN). Robustness of results was tested with a second model assuming exponentially distributed rates (uncorrelated exponentially distributed, UCED) (*SI Text*). For each clock model a set of eight different analyses were performed to take a broad range of prior assumptions into account and evaluate their influence on the results (Table 1 and Table S1). The Bayesian consensus tree of divergence-time analysis 7 is presented in Fig. 1, including age estimates (95% highest posterior densities, HPD) of important nodes as given by

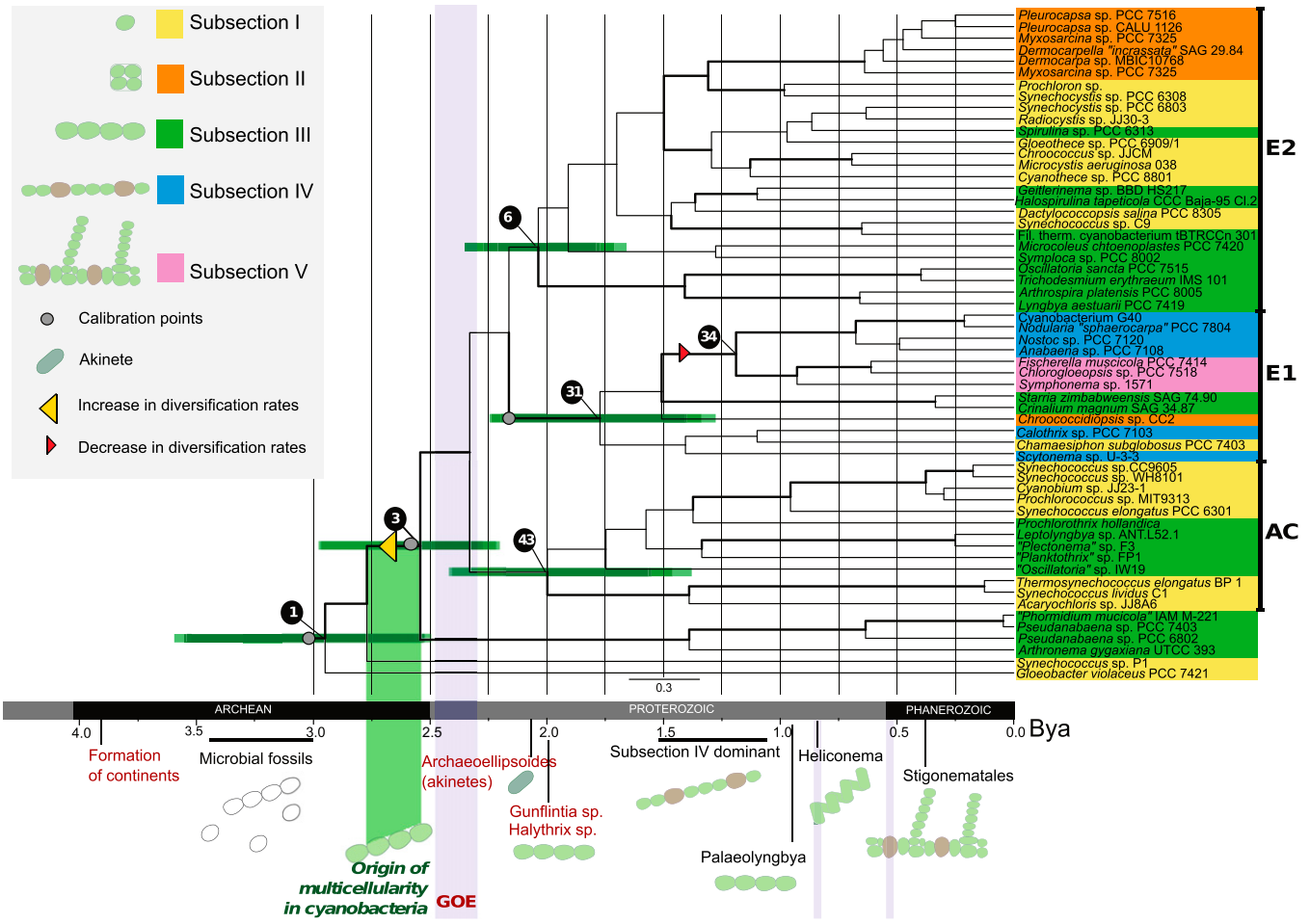

Fig. 1. Time calibrated phylogeny of cyanobacteria displaying divergence time estimates. Bayesian consensus tree (analysis 7) based on 16S rRNA data with 95% highest posterior densities of the discussed node ages shown as green bars (analyses 1, 3, 5, and 7 overlapping). Morphological features of taxa are marked by colored boxes and listed in the inset. Full taxon names are displayed in Table S3. Branches with posterior probabilities >0.9 in all analyses are presented as thick lines. Gray circles mark points used for calibration of the tree. Details of the prior age estimates used for calibration are presented in Table 1. A significant increase in diversification rate (yellow triangle) [9.66-fold (average of all analyses)] can be detected at node 3 and a minor decrease (red triangle) at 33/34. The earlier shift close to node 3 coincides with the origin of multicellularity. Schematic drawings of cyanobacterial fossils are provided under the timeline, with the ones used for calibration of the tree marked in red. Our results indicate that multicellularity (green shade) originated before or at the beginning of the GOE.

Table 1. Divergence times for five important nodes estimated using a relaxed clock with UCLN distributed evolutionary rates

Analysis	1	2	3	4	5	6	7	8
Model assumptions and calibration points								
Outgroup	No	No	Yes	Yes	Yes	Yes	No	No
Root	—	—	Exp(2.45;2.816)	Exp(2.45;2.816)	Exp(2.45;2.816)*	Exp(2.45;2.816)*	*	*
Node 3	LN(2.1;2.27,0.5)	LN(2.1;2.58,0.8)	LN(2.1;2.27,0.5)	LN(2.1;2.58,0.8)	LN(2.1;2.27,0.5)	LN(2.1;2.58,0.8)	LN(2.1;2.27,0.5)	LN(2.1;2.58,0.8)
Node 31 or 32	LN(2.1;2.13,1)	LN(2.1;2.13,1)	LN(2.1;2.13,1)	LN(2.1;2.13,1)	LN(2.1;2.13,1)	LN(2.1;2.13,1)	LN(2.1;2.13,1)	LN(2.1;2.13,1)
Results for discussed nodes (UCLN) $(\tilde{m})$(HPD) for all								
Node 1	2.95 (2.5–3.6)	3.67 (2.79–4.74)	2.99 (2.57–3.55)	3.35 (2.74–4.15)	2.87 (2.53–3.30)	3.06 (2.66–3.53)	2.95 (2.53–3.55)	3.39 (2.87–3.80)
Node 3	2.54 (2.28–2.98)	3.08 (2.42–3.84)	2.42 (2.21–2.73)	2.65 (2.28–3.18)	2.38 (2.20–2.62)	2.49 (2.26–2.81)	2.54 (2.29–2.97)	2.86 (2.43–3.34)
Node 6	2.04 (1.77–2.35)	2.33 (1.89–2.87)	2.02 (1.72–2.28)	2.10 (1.78–2.54)	1.99 (1.67–2.22)	2.02 (1.70–2.32)	2.04 (1.79–2.35)	2.18 (1.86–2.60)
Node 31	1.77 (1.4–2.24)	2.16 (1.53–2.56)	1.72 (1.34–2.20)	1.98 (1.39–2.34)	1.67 (1.28–2.17)	1.75 (1.30–2.23)	1.77 (1.41–2.25)	2.12 (1.50–2.41)
Node 43	2.00 (1.56–2.43)	2.35 (1.73–3.03)	1.85 (1.46–2.25)	1.97 (1.48–2.50)	1.80 (1.38–2.19)	1.86 (1.41–2.30)	2.00 (1.57–2.41)	2.18 (1.71–2.72)

Eight different combinations of calibration priors for the divergence time estimation were used. Exp, exponential distribution (offset;mean); LN, lognormal distribution (offset;mean, SD); —, calibration not applicable.
*Truncated at 3.8 Bya.

Fig. 2. Median age estimates under eight analytical scenarios. Median age estimates of clades (Table 1). The origin of cyanobacteria (node 1) and the evolution of multicellularity (node 3) are estimated before or at the beginning of the GOE. Relatively soon after the GOE, the stem lineages of the three major cyanobacterial clades originated, containing unicellular cyanobacteria (node 6), terminally differentiated taxa (node 31), and marine phycoplankton (node 43).

analyses 1, 3, 5, and 7 (Table 1). Median node ages $(\tilde{m})$ are shown in Fig. 2, and are provided with 95% HPD in Table 1 (discussed nodes) and Table S2 (all nodes). Although ages of cyanobacterial nodes varied with respect to the analyses, our major conclusions are robust to different calibration priors. All analyses indicated that extant cyanobacteria originated before the GOE (2.45 Bya). Multicellularity most likely originated along the branch leading to node 3 (5). For this node, analyses suggested a median age before or at the beginning of the GOE (before 2.36 Bya) (Table 1 and Table S1). The ancestor of the lineage leading to node 3 was also a calibration point in our analyses (Table 1). Fig. 3 compares the implied prior probability distributions of that calibration point to posterior probabilities of node 3, hence assessing the extent to which our prior assumptions affected the outcome. Although the prior assumptions put a higher probability on an age after the GOE around 2.2 Bya, our data contained strong signals to counteract these priors and indicate instead an older median node age for node 3, between 2.42–3.08 Bya (all analyses) (Fig. 3 and Table 1), which is before the GOE. Furthermore, groups E1, E2, and AC are estimated to have originated around the end of the GOE. These groups comprise the majority of living cyanobacteria (91% of 281 species and 88% of 4,194 strains).

Shifts in Diversification Rates. To identify whether the GOE or multicellularity might have influenced the net diversification of cyanobacteria, we tested whether diversification rates have been constant among cyanobacterial lineages. Because previous work suggested that taxonomy of cyanobacteria needed revision (1), we ran analyses incorporating information on both species (281) and strains (4,194). Clades containing many species also contain many strains (Table S3). Results from the diversification rate estimation showed similar patterns independent of whether species numbers or strain numbers were used (Table S4). Two significant shifts in diversification rates were detected. At node 3/4, where multicellularity evolved, the diversification rate increased on average 8.44-fold (SD = 1.76) for trees reconstructed with a UCLN model and 5.24-fold (SD = 1.89) for trees reconstructed with a UCED model (averaged over all analyses) (Table S4). Subsequently, at node 33/34, the diversification rate decreased by a factor of 0.55 (SD = 0.19) for trees reconstructed with a

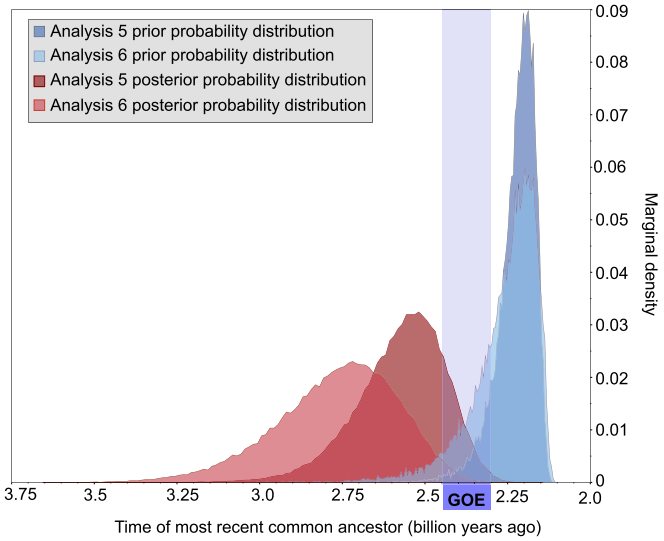

Fig. 3. Prior and posterior probability distributions of ages for node 3. Marginal prior probability distributions of analyses using narrow (analysis 5) and wide (analysis 6) prior distributions were conservatively biased toward younger ages, strongly favoring an origin of multicellularity after the GOE. Even so, posterior probabilities point to an origin of multicellularity before or at the beginning of the GOE, indicating that this main result is based on a strong signal in the data rather than a bias from a-priori assumptions. Marginal prior probability distributions were estimated in analyses that only sampled from the prior.

UCLN model, and by a factor of 0.22 (SD = 0.13) for trees reconstructed with a UCED model (Fig. 1 and Figs. S3–S6).

Discussion

Limitations of a Single Gene. The exchange of genetic material across species boundaries poses a challenge for the inference of evolutionary histories of living organisms (27–29). Phylogenetic reconstructions incorporating multiple genes help to reduce the danger to recover false signals from genes affected by horizontal gene transfer (HGT) (30, 31). Nevertheless, although genome data are accumulating, they do not nearly achieve the breadth of microbial diversity represented by 16S rRNA (32). 16S rRNA has been used as a reliable measure of phylogenetic relationship because of its size and conservation (33, 34, 35). These facts, in combination with a potentially smaller impact of HGT on genome evolution than commonly assumed, and even less on 16S rRNA (32, 36, 37), support the usefulness of the small ribosomal subunit for phylogenetic applications. Here we can neither exclude nor prove the possibility of 16S rRNA being affected by HGT between species. No cases have been found in support of HGT for 16S rRNA between cyanobacterial genera. We rely on 16S rRNA sequences in this study because a genomic approach would be biased toward unicellular taxa, would not cover the complete known diversity of this phylum and, hence, fail to reconstruct the early evolution of cyanobacteria (17). Nevertheless, we strongly encourage genome-sequencing projects that will help to recover the diversity indicated by 16S rRNA and improve reconstruction of a cyanobacterial phylogeny.

Evolution of Multicellularity and Possible Consequences. In prokaryotes simple forms of multicellularity occur in different phyla. In Actino- and Myxobacteria, multicellular growth formed via cell aggregation is part of their life cycle (38). In cyanobacteria, chloroflexi, and some proteobacteria (e.g., *Beggiatoa*) multicellularity is in a filamentous form. This result is achieved through cell division and adhesion, which results in filament elongation (39). Requirements for directed growth in filaments are cellular recognition of polarity (40) and cellular communication. Filamentous cyanobacteria, including simple forms like *Pseudanabaena* and *Leptolyngbya*, show directional growth where the plane of cell division depicts a right angle to the growth direction (1). In addition, intercellular communication and resource exchange has been found in cyanobacteria (41–43), providing an evolutionary basis for the division of labor and terminal cell differentiation to evolve (44–46).

Our results suggest a concurrence of the origin of multicellularity, the onset of the GOE, and an increased diversification rate of cyanobacteria; in addition, although their precise timing cannot be fully ascertained, they can be linked by theoretical and empirical lines of evidence. The transition to multicellularity represents an important change in organismic complexity (47). There are various advantages that multicellularity could confer (39, 48). Among others, filamentous growth can improve motility (49), and cooperation of cells may also increase fitness because of economies of scale. Experimental studies have shown that multicellularity might evolve relatively fast given selective pressure (50) and can provide metabolic fitness advantages compared with single cells (51). Increased fitness of multicellular species could have led to a higher frequency and wider distribution of cyanobacteria at the end of the Archean, consequently enhancing oxygen production. Accumulation of oxygen may have resulted in new ecological opportunities. Increased diversification rates around the time when multicellularity evolved suggest that cyanobacteria might have used, and possibly contributed to create, new adaptive opportunities. Subsequently, at the end of the GOE, three clades (E1, E2, and AC) evolved that led to the majority of cyanobacteria living today.

Early Earth History and the Fossil Record. Our finding that cyanobacteria have existed for a longer time than previously anticipated is congruent with reconstructions of early Earth history. The origin of Earth is deduced to date back ~4.5 Bya (52). Subsequently, the planet cooled down and eventually separated into core, mantle, and crust (53). Permanent existence of life before 4.2–3.8 Bya is unlikely, considering that the young Earth was subject to strong bombardment by asteroids (52, 54). Fossil evidence does not predate ~3.45 Bya (55, 56). Most of these prokaryotic fossils from the early Archean Eon have been identified in two regions: the Barberton Greenstone Belt (BGB), South Africa (around 3.20–3.50 billion y old), and the Pilbara Craton (PC), Western Australia (around 2.90–3.60 billion y old) (55–60). The oldest fossils from these regions are spherical, probably hyperthermophilic microbes [BGB (56, 59)] and filaments of possibly anoxygenic photosynthetic prokaryotes [East-PC (55, 56)], both around 3.45 billion y old. Further evidence for life includes 3.4 billion-y-old trace fossils (PC) (60), 3.42 billion-y-old deformed microbial mats (BGB) (57), and 3.0 billion-y-old biofilms (PC) (58). The earliest unequivocal cyanobacterial fossils date back around 2.0 Bya and come from two localities, the Gunflint iron formation and the Belcher Subgroup (both in Canada) (19, 20). Although differences in the microbial fossil composition have been recognized (19), both cherts include filamentous and coccoidal species. *Gunflintia grandis* and *Gunflintia minuta* have been identified as filamentous cyanobacterial fossils from the Gunflint iron formation, and *Halythrix* sp. has been described as an oscillatorian fossil from the Belcher subgroup (7) (Fig. 1). Cyanobacterial fossils younger than 2 billion y are more widely distributed (20), with various examples given in Fig. 1. Archean fossil findings may potentially depict remains of cyanobacteria but cannot be assigned beyond doubt (20). "Possible" cyanobacterial fossils have been found in 2.52–2.55 billion-y-old cherts in South Africa (20, 61). "Probable" unicellular and filamentous cyanobacterial fossils are distributed in 2.6 billion-y-old (20, 62–64) and 3.26 billion-y-old (64) cherts. Although previously described biomarkers that supported an existence of cyanobacteria around 2.7 Bya (65, 66) have been dismissed (67), recent evidence has been found in favor of an early cyanobacterial origin

(68–70). Our molecular dating results place the origin of both unicellular and multicellular cyanobacteria rather before the GOE, and thus suggest that some of those fossils could indeed represent relatives of cyanobacterial lineages.

Recent studies have suggested that oxygen accumulation occurred ~200–300 million y before the GOE (68, 69, 71). Current evidence from the fossil record, geochemical findings, and our molecular analyses, together support an origin of cyanobacteria clearly before the GOE. The origin of multicellularity toward the GOE could have entailed fitness advantages leading to an increase in cyanobacterial diversity and abundance, which in turn would positively influence net oxygen production.

Conclusion

Cyanobacteria are one of the morphologically most diverse prokaryotic phyla on this planet. It is widely accepted that they caused the GOE starting 2.45 Bya, but debates about their origin are still ongoing (67, 72, 73). Various lines of fossil and geochemical evidence have accumulated, supporting an origin of cyanobacteria before 2.45 Bya (20, 62, 64, 68–70). Here, we applied Bayesian phylogenetic analyses using relaxed molecular clocks and different combinations of calibration priors. We estimated the origin of extant cyanobacteria and their dominant morphotypes with respect to the GOE. Although resulting age estimates of the different analyses differ somewhat in their HPD, robust statements regarding the origin of cyanobacteria and their morphotypes can nevertheless be formulated: (*i*) cyanobacteria originated before the GOE, (*ii*) multicellularity coincides with the beginning of the rise of oxygen, and (*iii*) three clades representing the majority of extant cyanobacteria evolved shortly after the accumulation of atmospheric oxygen.

Materials and Methods

Taxon Sampling. Most sequences were downloaded from GenBank (74) (Table S3). Three eubacterial species were chosen as an outgroup: *Beggiatoa* sp., *Chlamydia trachomatis*, and *Spirochaeta thermophila*. A total of 58 cyanobacterial species were chosen for the analyses. Aside from strain G40 (*SI Text*) all taxa were selected as described previously (5). The taxa chosen comprise all morphological subsections described by Castenholz (1) and cover the morphological and genetic diversity of this phylum (5). Nomenclature and identity stated on GenBank might be incorrect. Therefore, we evaluated morphotypes (multicellular/unicellular) of each cyanobacterial strain by thoroughly examining the literature (Table S5) and conducting BLAST analyses, as described in *SI Text*. For most of those situations, full genome data are not yet available (17).

Alignment and Divergence Time Estimation. Sequence alignments were constructed using the program MUSCLE (Dataset S1) (75). Analyses were performed on datasets with outgroups [(*i*) 61 taxa, 1,090 sites, gaps excluded; 507 sites variable] and without outgroups [(*ii*) 58 taxa, 1,077 sites, gaps excluded; 421 sites variable]. Uncorrected and corrected Akaike Information Criterion (76, 77), implemented in jModelTest v0.1.1 (78), suggested a general time-reversible substitution model with γ-distributed rate variation among sites (GTR+G) (79) as the most suitable model of sequence evolution. Phylogenetic analyses using Bayesian inference were conducted as described in *SI Text*. We applied relaxed clocks with UCLN and UCED rate distributions (Table 1 and Table S1) (80). The analyses were conducted with a combination of three calibration points. Additionally, monophyly constraints were set for three nodes that were supported by our previous Bayesian phylogenetic analyses (Fig. S1 and *SI Text*): (*i*) the phylum cyanobacteria, (*ii*) cyanobacteria, excluding *Gloeobacter*, and (*iii*) cyanobacteria excluding *Synechococcus* sp. P1 and *Gloeobacter* (Fig. 1). The phylum cyanobacterian (*i*) has been extensively investigated and confirmed before [i.e., cyanobacteria as a monophyletic group within the Eubacteria (5)]. For cyanobacteria, excluding *Gloeobacter* (*ii*), an early divergence of *Gloeobacter* has been supported in previous analyses (5, 17, 24). Unlike other cyanobacteria, *G. violaceus* lacks thylacoid membranes (81), and various differences in gene content compared with cyanobacteria have been found (82). For cyanobacteria excluding *Synechococcus* sp. P1 and *Gloeobacter* (*iii*), *Synechococcus* sp. P1 is a thermophilic unicellular cyanobacterium isolated from Octopus Spring in Yellowstone nationalpark (83). Its proximity to *Gloeobacter* and eubacterial outgroups has been shown by genetic comparisons and phylogenetic analyses (5, 17, 24). Divergence time estimation was conducted using the software BEAST v1.6.2 (80) and run on the CIPRES Science Gateway v.3.1 (84). For each analysis, we ran six Markov chain Monte Carlo chains for 50-million generations, sampling every 2,000th generation (input files provided as Dataset S2). Although convergence of all parameters was reached before 5 million generations, we excluded a conservative 25% initial burn-in. Results are presented on a 50% majority-rule consensus tree calculated with SumTrees v3.3.1 (85).

Calibration Points. ***The root: Stem lineage of cyanobacteria.*** Four of the eight divergence time analyses included an outgroup (Table 1: analyses 3, 4, 5, 6), which enabled calibrating the cyanobacterial stem lineage. The GOE dates back 2.32–2.45 billion y (9), and is assumed to be a result of cyanobacterial activity. We use the start of the GOE as the minimum date for the divergence of cyanobacterial stem lineage and the outgroup. The possibility of permanently existing lifeforms is suggested to occur earliest around 3.8 Bya (52), which we used as earliest date (i.e., maximum age) of our root calibration. See Table 1 for a detailed description of prior age probability distributions. For analyses 7 and 8, the age of the earliest split of cyanobacteria, namely between *Gloeobacter* and the rest of cyanobacteria, was accordingly restricted to 3.8–2.45 Bya.

Node 3: First multicellular cyanobacteria. Node 3 in Fig. 1 was estimated to be a multicellular ancestor of extant cyanobacteria, as recovered previously (5). Fossil records indicate that terminally differentiated cyanobacteria (subsections IV and V) evolved before 2.1 Bya. Such differentiation may only evolve in a multicellular setting (44). We therefore assume that the stem lineage of node 3 must have been present before 2.1 Bya, and use this as a hard minimum bound of a lognormal prior distribution. We used a soft upper bound, linking the distribution of prior probabilities to the timing of the GOE. Multicellularity may have evolved as a consequence of new habitats that became available after the GOE, 2.3 Bya, or it could instead have triggered a rise of oxygen in the atmosphere. Therefore, we distinguish two calibration scenarios, one by setting the probability of the age of node 3 to a lognormal distribution with 95% being younger than 2.45 (Table 1: analyses 1, 3, 5), and the other by setting the median age of the before 2.45 Bya (Table 1: analyses 2, 4, 6).

Node 31 or 32: First terminally differentiated cyanobacteria. Cyanobacteria belonging to subsection IV and V share the property to form resting cells named akinetes. Fossilized remains of these akinetes have been identified at various locations throughout the Proterozoic (6, 19, 86). The oldest of these fossilized akinetes are found in 2.1 billion-y-old rocks (6, 13), and imply that cyanobacteria belonging to subsection IV and V originated before 2.1 Bya. Taxa of this group are capable of terminal cell differentiation. Oxygen sensitive nitrogen fixation is spatially separated from oxygenic photosynthesis and takes place in so called heterocysts. Oxygen levels providing a selective advantage for separation of these processes were reached ~2.45 Bya (13). As a calibration for the divergence time estimation, we set the most recent common ancestor of taxa from subsections IV and V to 2.1 billion y as a hard minimum bound, and specified 95% of prior probabilities before 2.45 Bya, using a lognormal distribution.

Shifts in Diversification Rates. To test whether the rate of lineage accumulation has been constant throughout cyanobacterial evolution, we used the function MEDUSA from the geiger 1.3-1 package in R (87). We corrected for possible taxon sampling biases by including information on known numbers of extant species and strains, which were collected from GenBank. Details are given in *SI Text* and Table S3. MEDUSA was run based on 50% majority-rule consensus trees calculated with SumTrees v3.3.1 (85), derived from the eight BEAST analyses (Table 1).

ACKNOWLEDGMENTS. We thank Akos Dobay, Valentina Rossetti, Manuela Filippini-Cattani, the editor S.G., and three anonymous reviewers for helpful comments on the manuscript. This work was supported in part by Canton of Zurich; A.A. is supported by grants from the Swedish and the European Research Councils. B.E.S. is supported by the Swiss National Science Foundation.

1. Boone DR, Castenholz RW (2001) *Bergey's Manual of Systematic Bacteriology: The Archaea and the Deeply Branching and Phototropic Bacteria: Cyanobacteria*, ed Garrity GM (Springer, New York).
2. Rippka R, Deruelles J, Waterbury JB, Herdman M, Stanier RY (1979) Generic assignments, strain histories and properties of pure cultures of cyanobacteria. *J Genl MicrobioLogy* 111: 1–61.
3. Giovannoni SJ, et al. (1988) Evolutionary relationships among cyanobacteria and green chloroplasts. *J Bacteriol* 170(8):3584–3592.
4. Gugger MF, Hoffmann L (2004) Polyphyly of true branching cyanobacteria (Stigonematales). *Int J Syst Evol Microbiol* 54(Pt 2):349–357.
5. Schirrmeister BE, Antonelli A, Bagheri HC (2011) The origin of multicellularity in cyanobacteria. *BMC Evol Biol* 11:45.

6. Amard B, Bertrand-Sarfati J (1997) Microfossils in 2000 ma old cherty stromatolites of the Franceville group, Gabon. *Precambrian Res* 81(3–4):197–221.
7. Hofmann HJ (1976) Precambrian Microflora, Belcher islands, Canada—Significance and systematics. *J Paleontol* 50(6):1040–1073.
8. Blankenship RE (2002) *Molecular Mechanisms of Photosynthesis* (Blackwell Science, Oxford).
9. Bekker A, et al. (2004) Dating the rise of atmospheric oxygen. *Nature* 427(6970):117–120.
10. Kopp RE, Kirschvink JL, Hilburn IA, Nash CZ (2005) The Paleoproterozoic snowball Earth: A climate disaster triggered by the evolution of oxygenic photosynthesis. *Proc Natl Acad Sci USA* 102(32):11131–11136.
11. Allen JF, Martin W (2007) Evolutionary biology: Out of thin air. *Nature* 445(7128):610–612.
12. Frei R, Gaucher C, Poulton SW, Canfield DE (2009) Fluctuations in Precambrian atmospheric oxygenation recorded by chromium isotopes. *Nature* 461(7261):250–253.
13. Tomitani A, Knoll AH, Cavanaugh CM, Ohno T (2006) The evolutionary diversification of cyanobacteria: Molecular-phylogenetic and paleontological perspectives. *Proc Natl Acad Sci USA* 103(14):5442–5447.
14. Battistuzzi FU, Hedges SB (2009) A major clade of prokaryotes with ancient adaptations to life on land. *Mol Biol Evol* 26(2):335–343.
15. Blank CE, Sánchez-Baracaldo P (2010) Timing of morphological and ecological innovations in the cyanobacteria—A key to understanding the rise in atmospheric oxygen. *Geobiology* 8(1):1–23.
16. Larsson J, Nylander JAA, Bergman B (2011) Genome fluctuations in cyanobacteria reflect evolutionary, developmental and adaptive traits. *BMC Evol Biol* 11:187.
17. Schirrmeister BE, Anisimova M, Antonelli A, Bagheri HC (2011) Evolution of cyanobacterial morphotypes: Taxa required for improved phylogenomic approaches. *Commun Integr Biol* 4(4):424–427.
18. Wu DY, et al. (2009) A phylogeny-driven genomic encyclopaedia of Bacteria and Archaea. *Nature* 462(7276):1056–1060.
19. Golubic S, Lee SJ (1999) Early cyanobacterial fossil record: Preservation, palaeoenvironments and identification. *Eur J Phycol* 34(4):339–348.
20. Sergeev VN, Gerasimenko LM, Zavarzin GA (2002) [Proterozoic history and present state of cyanobacteria]. *Mikrobiologiia* 71(6):725–740.
21. Benton MJ (2003) The quality of the fossil record. *Telling the Evolutionary Time: Molecular Clocks and the Fossil Record*, eds Donoghue PCJ, Smith MP (Tayler & Francis, London), pp 66–90.
22. Reisz RR, Müller J (2004) Molecular timescales and the fossil record: A paleontological perspective. *Trends Genet* 20(5):237–241.
23. Donoghue PCJ, Benton MJ (2007) Rocks and clocks: Calibrating the Tree of Life using fossils and molecules. *Trends Ecol Evol* 22(8):424–431.
24. Turner S, Pryer KM, Miao VPW, Palmer JD (1999) Investigating deep phylogenetic relationships among cyanobacteria and plastids by small subunit rRNA sequence analysis. *J Eukaryot Microbiol* 46(4):327–338.
25. Honda D, Yokota A, Sugiyama J (1999) Detection of seven major evolutionary lineages in cyanobacteria based on the 16S rRNA gene sequence analysis with new sequences of five marine *Synechococcus* strains. *J Mol Evol* 48(6):723–739.
26. Drummond AJ, Ho SYW, Phillips MJ, Rambaut A (2006) Relaxed phylogenetics and dating with confidence. *PLoS Biol* 4(5):e88.
27. Doolittle WF (1999) Phylogenetic classification and the universal tree. *Science* 284 (5423):2124–2129.
28. Gogarten JP, Doolittle WF, Lawrence JG (2002) Prokaryotic evolution in light of gene transfer. *Mol Biol Evol* 19(12):2226–2238.
29. Andam CP, Gogarten JP (2011) Biased gene transfer in microbial evolution. *Nat Rev Microbiol* 9(7):543–555.
30. Suchard MA (2005) Stochastic models for horizontal gene transfer: Taking a random walk through tree space. *Genetics* 170(1):419–431.
31. Lapierre P, Lasek-Nesselquist E, Gogarten JP (2012) The impact of HGT on phylogenomic reconstruction methods. *Brief Bioinform*, 10.1093/bib/bbs050.
32. Yarza P, et al. (2008) The All-Species Living Tree project: A 16S rRNA-based phylogenetic tree of all sequenced type strains. *Syst Appl Microbiol* 31(4):241–250.
33. Woese CR (1987) Bacterial evolution. *Microbiol Rev* 51(2):221–271.
34. Olsen GJ, Woese CR (1993) Ribosomal RNA: A key to phylogeny. *FASEB J* 7(1):113–123.
35. Schirrmeister BE, Dalquen DA, Anisimova M, Bagheri HC (2012) Gene copy number variation and its significance in cyanobacterial phylogeny. *BMC Microbiol* 12(1):177.
36. Snel B, Bork P, Huynen MA (2002) Genomes in flux: The evolution of archaeal and proteobacterial gene content. *Genome Res* 12(1):17–25.
37. Kurland CG, Canback B, Berg OG (2003) Horizontal gene transfer: A critical view. *Proc Natl Acad Sci USA* 100(17):9658–9662.
38. Rokas A (2008) The molecular origins of multicellular transitions. *Curr Opin Genet Dev* 18(6):472–478.
39. Rossetti V, Filippini M, Svercel M, Barbour AD, Bagheri HC (2011) Emergent multicellular life cycles in filamentous bacteria owing to density-dependent population dynamics. *J R Soc Interface* 8(65):1772–1784.
40. Knoll AH, Javaux EJ, Hewitt D, Cohen P (2006) Eukaryotic organisms in Proterozoic oceans. *Philos Trans R Soc Lond B Biol Sci* 361(1470):1023–1038.
41. Giddings TH, Staehelin LA (1981) Observation of Microplasmodesmata in both heterocyst-forming and non-heterocyst forming filamentous Cyanobacteria by freeze-fracture electron microscopy. *Arch Microbiol* 129(4):295–298.
42. Flores E, Herrero A, Wolk CP, Maldener I (2006) Is the periplasm continuous in filamentous multicellular cyanobacteria? *Trends Microbiol* 14(10):439–443.
43. Flores E, Herrero A (2010) Compartmentalized function through cell differentiation in filamentous cyanobacteria. *Nat Rev Microbiol* 8(1):39–50.
44. Rossetti V, Schirrmeister BE, Bernasconi MV, Bagheri HC (2010) The evolutionary path to terminal differentiation and division of labor in cyanobacteria. *J Theor Biol* 262(1):23–34.
45. Ispolatov I, Ackermann M, Doebeli M (2012) Division of labour and the evolution of multicellularity. *Proc Biol Sci* 279(1734):1768–1776.
46. Rossetti V, Bagheri HC (2012) Advantages of the division of labour for the long-term population dynamics of cyanobacteria at different latitudes. *Proc Biol Sci* 279(1742): 3457–3466.
47. Maynard Smith J, Szathmary E (1995) *The Major Transitions in Evolution*. (Oxford University Press, Oxford).
48. Bonner J (1998) The origin of multicellularity. *Integr Biol* 1(1):28–36.
49. Adams DG (1997) *Cyanobacteria. Bacteria as Multicellular Organism*, eds Shapiro JA, Dworkin M (Oxford Univ Press, New York), pp 109–148.
50. Ratcliff WC, Denison RF, Borrello M, Travisano M (2012) Experimental evolution of multicellularity. *Proc Natl Acad Sci USA* 109(5):1595–1600.
51. Koschwanez JH, Foster KR, Murray AW (2011) Sucrose utilization in budding yeast as a model for the origin of undifferentiated multicellularity. *PLoS Biol* 9(8):e1001122.
52. Nisbet EG, Sleep NH (2001) The habitat and nature of early life. *Nature* 409(6823): 1083–1091.
53. Mojzsis SJ (2010) Early earth leftover lithosphere. *Nat Geosci* 3:148–149.
54. Sleep NH, Zahnle KJ, Kasting JF, Morowitz HJ (1989) Annihilation of ecosystems by large asteroid impacts on the early Earth. *Nature* 342(6246):139–142.
55. Westall F, et al. (2006) The 3.466 ga "Kitty's gap chert" an early Archean microbial ecosystem. *Spec Pap Geol Soc Am* 405:105–131.
56. Wacey D (2009) *Early Life on Earth: A Practical Guide* (Springer, New York).
57. Tice MM, Lowe DR (2004) Photosynthetic microbial mats in the 3,416-Myr-old ocean. *Nature* 431(7008):549–552.
58. Sugitani K, et al. (2007) Diverse microstructures from Archaean chert from the mount Goldsworthy-mount grant area, Pilbara Craton, Western Australia: Microfossils, dubiofossils, or pseudofossils? *Precambrian Res* 158:228–262.
59. Glikson M, et al. (2008) Microbial remains in some earliest Earth rocks: Comparison with a potential modern analogue. *Precambrian Res* 164(3–4):187–200.
60. Wacey D, et al. (2008) Use of nanosims in the search for early life on Earth: Ambient inclusion trails in a c. 3400 ma sandstone. *J Geol Soc London* 165(1):43–53.
61. Knoll AH (1996) *Palynology: Principles and Applications–Archean and Proterozoic Paleontology*. (American Association of Stratigraphic Palynologists, Tulsa, OK), pp 51–80.
62. Altermann W, Schopf JW (1995) Microfossils from the Neoarchean Campbell Group, Griqualand west sequence of the Transvaal Supergroup, and their paleoenvironmental and evolutionary implications. *Precambrian Res* 75(1–2):65–90.
63. Kazmierczak J, Altermann W (2002) Neoarchean biomineralization by benthic cyanobacteria. *Science* 298(5602):2351.
64. Schopf JW (2009) Paleontology, microbial. *Encyclopedia of Microbiology*, eds Lederberg J, Schaechter M (Elsevier, Amsterdam), 3rd Ed, pp 390—400.
65. Brocks JJ, Logan GA, Buick R, Summons RE (1999) Archean molecular fossils and the early rise of eukaryotes. *Science* 285(5430):1033–1036.
66. Summons RE, Jahnke LL, Hope JM, Logan GA (1999) 2-Methylhopanoids as biomarkers for cyanobacterial oxygenic photosynthesis. *Nature* 400(6744):554–557.
67. Rasmussen B, Fletcher IR, Brocks JJ, Kilburn MR (2008) Reassessing the first appearance of eukaryotes and cyanobacteria. *Nature* 455(7216):1101–1104.
68. Lyons TW, Reinhard CT (2011) Earth science: Sea change for the rise of oxygen. *Nature* 478(7368):194–195.
69. Gaillard F, Scaillet B, Arndt NT (2011) Atmospheric oxygenation caused by a change in volcanic degassing pressure. *Nature* 478(7368):229–232.
70. Waldbauer JR, Sherman LS, Sumner DY, Summons RE (2009) Late Archean molecular fossils from the Transvaal Supergroup record the antiquity of microbial diversity and aerobiosis. *Precambrian Res* 169(1–4):28–47.
71. Stüeken EE, Catling DC, Buick R (2012) Contributions to late Archaean sulphur cycling by life on land. *Nat Geosci* 5(10):722—725.
72. Schopf JW (1993) Microfossils of the Early Archean Apex chert: New evidence of the antiquity of life. *Science* 260(5108):640–646.
73. Brasier M, McLoughlin N, Green O, Wacey D (2006) A fresh look at the fossil evidence for early Archaean cellular life. *Philos Trans R Soc Lond B Biol Sci* 361(1470):887–902.
74. Bilofsky HS, Burks C (1988) The GenBank genetic sequence data bank. *Nucleic Acids Res* 16(5):1861–1863.
75. Edgar RC (2004) MUSCLE: multiple sequence alignment with high accuracy and high throughput. *Nucleic Acids Res* 32(5):1792–1797.
76. Akaike H (1974) New look at statistical-model identification. *IEEE Trans Automat Contr* AC19(6):716–723.
77. Hurvich CM, Tsai CL (1989) Regression and time-series model selection in small samples. *Biometrika* 76(2):297–307.
78. Posada D (2008) jModelTest: Phylogenetic model averaging. *Mol Biol Evol* 25(7):1253–1256.
79. Lanave C, Preparata G, Saccone C, Serio G (1984) A new method for calculating evolutionary substitution rates. *J Mol Evol* 20(1):86–93.
80. Drummond AJ, Rambaut A (2007) BEAST: Bayesian evolutionary analysis by sampling trees. *BMC Evol Biol* 7:214.
81. Rippka R, Waterbury J, Cohenbazire G (1974) Cyanobacterium which lacks thylakoids. *Arch Microbiol* 100(1):419–436.
82. Nakamura Y, et al. (2003) Complete genome structure of *Gloeobacter violaceus* PCC 7421, a cyanobacterium that lacks thylakoids. *DNA Res* 10(4):137–145.
83. Ferris MJ, Ruff-Roberts AL, Kopczynski ED, Bateson MM, Ward DM (1996) Enrichment culture and microscopy conceal diverse thermophilic *Synechococcus* populations in a single hot spring microbial mat habitat. *Appl Environ Microbiol* 62(3):1045–1050.
84. Miller M, et al. (2009) The CIPRES portals. CIPRES. Available at. www.phyloorg/sub_sections/portal. Accessed February 2012.
85. Sukumaran J, Holder MT (2010) DendroPy: A Python library for phylogenetic computing. *Bioinformatics* 26(12):1569–1571.
86. Golubic S, Sergeev VN, Knoll AH (1995) Mesoproterozoic Archaeoellipsoides: Akinetes of heterocystous cyanobacteria. *Lethaia* 28:285–298.
87. Alfaro ME, et al. (2009) Nine exceptional radiations plus high turnover explain species diversity in jawed vertebrates. *Proc Natl Acad Sci USA* 106(32):13410–13414.